Multiferroic properties of uniaxially compressed orthorhombic $HoMnO_3$ thin films

K. Shimamoto,[1] Y. W. Windsor,[2] Y. Hu,[1] M. Ramakrishnan,[2] A. Alberca,[2] E. M. Bothschafter,[2] L. Rettig,[2] Th. Lippert,[1,3] U. Staub,[2] and C. W. Schneider[1]
[1]*Energy and Environment Research Division, Paul Scherrer Institut, CH 5232 Villigen-PSI, Switzerland*
[2]*Swiss Light Source, Paul Scherrer Institut, CH 5232 Villigen-PSI, Switzerland*
[3]*Department of Chemistry and Applied Biosciences, Laboratory of Inorganic Chemistry, ETH Zurich, CH 8093 Zurich, Switzerland*

(Received 21 December 2015; accepted 26 February 2016; published online 18 March 2016)

Multiferroic properties of orthorhombic $HoMnO_3$ (*Pbnm* space group) are significantly modified by epitaxial compressive strain along the *a*-axis. We are able to focus on the effect of strain solely along the *a*-axis by using an $YAlO_3$ (010) substrate, which has only a small lattice mismatch with $HoMnO_3$ along the other in-plane direction (the *c*-axis). Multiferroic properties of strained and relaxed $HoMnO_3$ thin films are compared with those reported for bulk, and are found to differ widely. A relaxed film exhibits bulk-like properties such as ferroelectricity below 25 K and an incommensurate antiferromagnetic order below 39 K, with an ordering wave vector of $(0\ q_b\ 0)$ with $q_b \approx 0.41$ at ~10 K. A strained film becomes ferroelectric already at 37.5 K and has an incommensurate magnetic order with $q_b \approx 0.49$ at ~10 K. © *2016 AIP Publishing LLC*.
[http://dx.doi.org/10.1063/1.4944460]

Heteroepitaxial growth of oxide materials has been an attractive topic over the past few decades, opening new research fields in electronics and spintronics. To cultivate potential applications, growth of oxide films with electric and magnetic orders (multiferroics) is an attempt to achieve control of magnetic properties via electric fields, and vice versa.[1–4] Upon deposition, thin films are forced to grow on substrates in an energetically favorable manner, thereby epitaxial strain is introduced. Since the interatomic distances in the material are altered, physical properties of a film can differ from those of bulk. When a film exceeds a certain threshold thickness (critical thickness), it exhibits lattice relaxation by introducing defects that allow the lattice constants to approach bulk values.[5–9] Many physical properties can be altered accordingly. For example, the transition temperature of ferromagnetic or ferroelectric (FE) orders can drastically change, as can the magnitude of the associated order parameter.[10–13] Furthermore, when epitaxial strain is applied to a material which is close to a magnetic and/or electric phase boundary, the ordering motif itself can be changed.[14–16]

The orthorhombic rare-earth manganites (*o*-$REMnO_3$, RE = Tb–Lu, Y, *Pbnm* space group) are multiferroics with strong magnetoelectric coupling.[17,18] This series of materials can be roughly categorized according to two ground states: a *bc*-cycloidal magnetic phase with a *c*-axis FE polarization, and an E-type magnetic phase whose FE polarization is expected along the *a*-axis.[19] *o*-$HoMnO_3$ (*o*-HMO) and *o*-$YMnO_3$ (*o*-YMO) sit at the boundary between these phases, exhibiting different magnetic and electric properties depending on the synthesis method (Ho: Refs. 20–26, Y: Refs. 22, 23, and 26–29). This indicates that these two materials are sensitive to perturbations. There are several reports on the effects of epitaxial strain on *o*-YMO. For example, when grown coherently on a (010) oriented $YAlO_3$ (YAO (010)) substrate, *o*-YMO films exhibit two electric transitions at 40 and 30 K,[30] while bulk exhibits only one at 30 K.[28] Magnetic and electric properties change significantly when *o*-YMO is grown on $SrTiO_3$ substrates.[31–33]

In this report, we focus on epitaxial films of *o*-HMO ($a = 5.2572$ Å, $b = 5.8354$ Å, and $c = 7.3606$ Å)[34] on YAO ($a = 5.1796$ Å, $b = 5.3286$ Å, and $c = 7.3706$ Å)[35] (010) substrates (Crystec Co., Ltd.), which have an in-plane lattice mismatch of 1.48% (compressive) along the *a*-axis and −0.14% (tensile) along the *c*-axis. Due to the large lattice mismatch between *o*-HMO and YAO, we expect that the films will relax when they are sufficiently thick. Our study is designed to identify differences in electric and magnetic properties between coherently grown and fully relaxed *o*-HMO.

o-HMO films were grown by pulsed laser deposition. Pulsed beams from a KrF excimer laser ($\lambda = 248$ nm) were focused onto a hexagonal HMO target with a fluence of 2.7 J cm^{-2} in a N_2O partial pressure of 0.30 mbar. The substrate temperature was maintained at 780 °C by a Si resistive heater with a target-substrate distance of 37 mm. Film thickness was varied from 20 to 400 nm to investigate the effect of epitaxial strain. Lattice parameters were determined with a four-circle x-ray diffractometer. Capacitance measurements were performed by an Agilent E4980A LCR meter with an AC voltage of 100 mV and FE hysteresis was probed through the Positive-Up Negative-Down (double-wave) method.[36] Magnetic order was probed by resonant soft x-ray diffraction (RSXD) using the RESOXS UHV diffraction end station[37] at the SIM beam line[38] of the Swiss Light Source (SLS), with applied photon energies of ~643 eV corresponding to the Mn L_3 absorption edge, providing element-sensitivity and resonant enhancement of the magnetic signal. Other experimental details are described elsewhere.[39]

The out-of-plane $\theta - 2\theta$ scan of a 400 nm film shown in Fig. 1(a) indicates that the HMO film is in the orthorhombic

phase. Reciprocal space maps (RSM) of the (130) and (041) reflections from *o*-HMO films with various thicknesses are shown in Figs. 1(b) and 1(c), respectively. RSMs from a 20 nm *o*-HMO film clearly demonstrate that the film is coherently grown, and is strained by 1.48% (compressive) along the *a*- and −0.14% (tensile) along the *c*-axis. For films thicker than 100 nm, two distinct (130) reflections were observed, demonstrating that the thick *o*-HMO films experience strain relaxation. The critical thickness of an *o*-HMO film on a YAO (010) substrate is ∼30 nm for the aforementioned growth condition, considering that the (130) reflection from a 32 nm *o*-HMO film starts to broaden towards the bulk position (see Fig. 1(b)). To roughly illustrate this behavior, a schematic cross section of the *o*-HMO film along the *a*-axis is shown in Fig. 1(d). When an *o*-HMO film is grown thicker than the critical thickness, a relaxed layer starts to form on top of the strained one. The broadened diffraction peak of the relaxed layer indicates that this layer has more defects due to strain relaxation. The RSMs in Figs. 1(b) and 1(c) show that the diffraction peaks from the relaxed layer shift towards bulk values with growing thickness. Furthermore, the lattice constants measured for both layers (Fig. 1(e)) indicate that the relaxed layer converges to bulk values up to 200 nm, above which the strain is fully relaxed. Here, we note that the shift of the *a*-axis lattice parameter due to strain relaxation is observed only in the relaxed layer. The change in the *c*-axis lattice parameter is small compared to that in the *a*-axis. It is therefore reasonable to consider that differences between the strained and the relaxed *o*-HMO layers originate from the compressive strain along the *a*-axis.

Electric properties of *o*-HMO films were characterized with Au (56 nm)/Ti (4 nm) interdigitated electrodes patterned on the film surface (Fig. 2(a)). The electrodes were aligned with respect to the crystallographic in-plane axes of the film, i.e., *a*- and *c*-axis. Dielectric properties of 20 nm and 200 nm *o*-HMO films are shown in Fig. 2. A small dielectric loss ($\tan\delta < 0.005$, Figs. 2(c) and 2(e)) demonstrates that both samples are well insulating. A larger dielectric loss in the 200 nm film is due to larger mosaicity in the relaxed layer (Figs. 1(b) and 1(c)), which induces small defect conductance.

The FE transition temperature (T_{FE}) of the 20 nm film is 37.5 K as determined from the temperature dependence of the normalized capacitance ($\Delta C(T)$) along the *a*-axis (Fig. 2(b)). No pronounced transition was observed along the *c*-axis. Unlike in the case of the *o*-YMO film on YAO (010),[30] only one transition was observed. A small thermal hysteresis of the $\Delta C(T)$ indicates a weak first order nature of the FE transition (Fig. 2(b)). These dielectric properties of the strained *o*-HMO film are different from any of the reported bulk *o*-HMO results[20–22] but are close to those of *o*-*RE*MnO_3 with smaller *RE* ions such as Tm[40] and Lu.[41]

The 200 nm film exhibited different dielectric properties compared to the strained 20 nm film (Figs. 2(d) and 2(e)). The $\Delta C(T)$ along the *a*-axis starts to increase at around 42 K, showing a small hump at ∼37 K, which corresponds to the FE transition of the strained layer (cf. Fig. 1(d)). It then exhibits a rounded peak and thermal hysteresis, with a crossing between cooling and heating measurements at around 21 K. This behavior is similar to polycrystalline bulk samples reported by Lorenz *et al.*[22] The ΔC along the *c*-axis exhibits

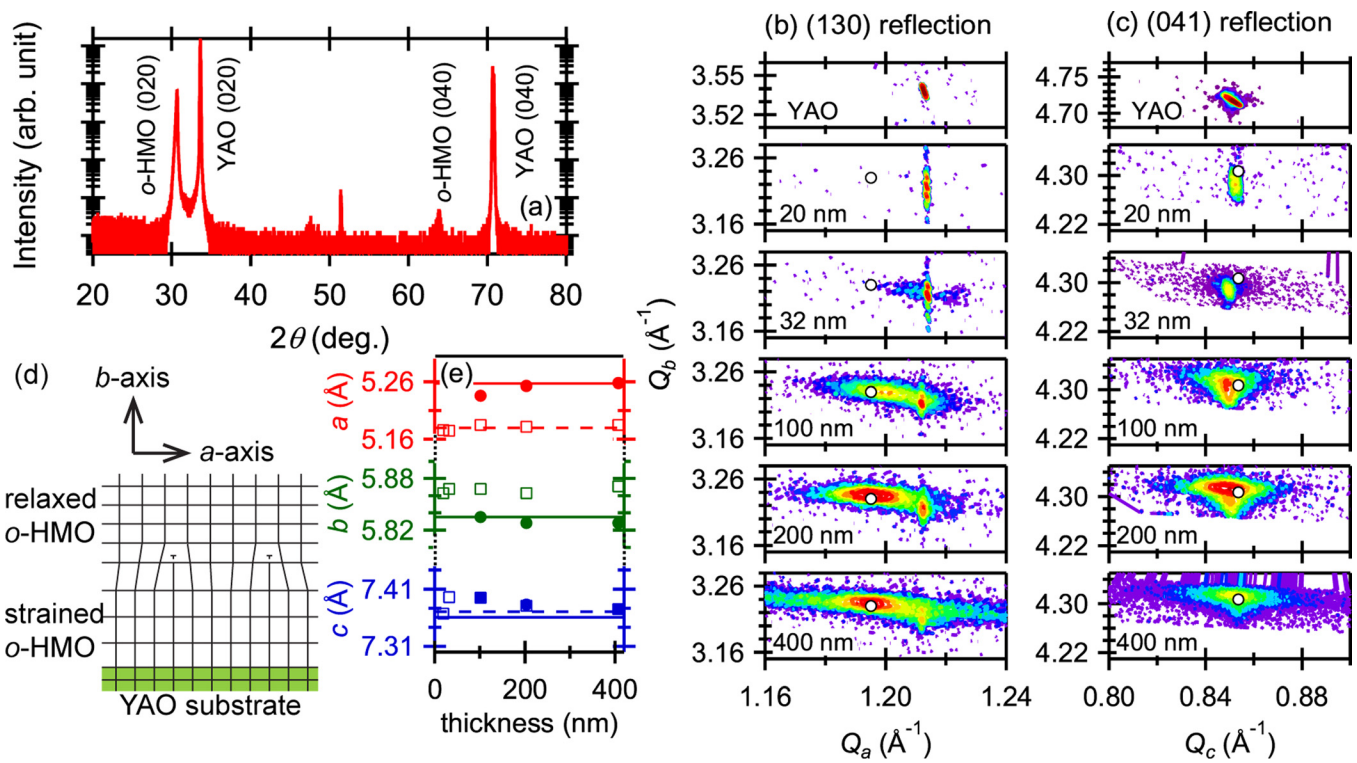

FIG. 1. (a) $\theta - 2\theta$ scan of a 400 nm *o*-HMO film. (b) and (c) Reciprocal space maps around the (130) and (041) reflections (respectively) of *o*-HMO films of various thicknesses. A white marker indicates the position for bulk *o*-HMO. (d) Schematic side-view of the relaxed and the strained layers of the film. (e) Lattice parameters of *o*-HMO films (open symbols: strained layer, closed symbols: relaxed layer) derived from (b) and (c). Horizontal solid and dashed lines indicate the values of *o*-HMO[34] and of YAO,[35] respectively.

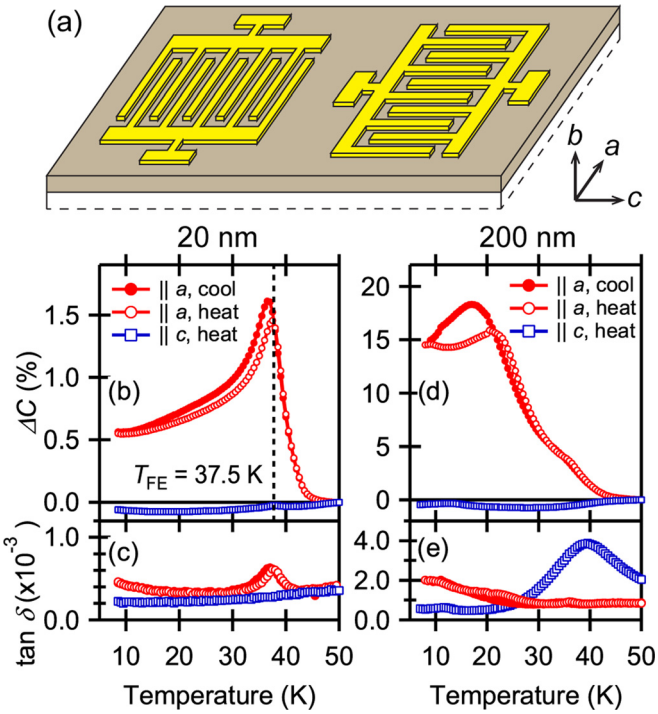

FIG. 2. (a) A schematic image of patterned interdigitated electrodes. Temperature dependent electric properties of (b) and (c) the 20 nm and (d) and (e) the 200 nm *o*-HMO films: (b) and (d) normalized capacitance and (c) and (e) loss tangent. The normalized capacitance is derived by $\Delta C = (C(T) - C(50\,\mathrm{K}))/C(50\,\mathrm{K})$.

a smaller response to the change of temperature than along the *a*-axis. The FE transition of the relaxed layer is not straightforward to interpret as $\Delta C(T)$ does not show a clear divergent behavior, an indication of a FE transition in the conventional Landau theoretical framework.

Ferroelectric hysteresis curves were measured upon heating, settling at each measurement temperature. The effective polarization (P_{eff}) was calculated as $P_{\mathrm{eff}} = Q(tL)^{-1}$, where Q is the measured charge, t the film thickness, and L the total length of the finger pairs.[42–44] The effective remnant polarization ($P_{\mathrm{r\text{-}eff}}$) was derived from the measured FE hysteresis curves (e.g., Fig. 3(a) inset) at each temperature. The temperature dependent $P_{\mathrm{r\text{-}eff}}$ of the 20 nm film probed by a poling field (E_{pol}) of 47 kV cm^{-1} appears below T_{FE}, and reaches ~130 nC cm^{-2} at low temperatures. The drop in remnant polarization below ~20 K is due to the limited input voltage experimentally available, which is too weak to fully polarize the sample at lower temperatures.

The FE properties of the 200 nm film are shown in Figs. 3(b) and 3(c). A FE hysteresis curve probed with $E_{\mathrm{pol}} = 47$ kV cm^{-1} measured along the *a*-axis at 10 K exhibits a superposition of two FE components (Fig. 3(b) inset). These two are attributed to the relaxed and strained layers (cf. Fig. 1(d)). To understand the FE transition of the relaxed layer, we focus on the temperature dependence of $P_{\mathrm{r\text{-}eff}}$, taken with $E_{\mathrm{pol}} = 15$ kV cm^{-1} (Fig. 3(c)) which is immediately above the onset of the $P_{\mathrm{r\text{-}eff}}$ vs. E_{pol} curve at 10 K (Fig. 3(c) inset). $P_{\mathrm{r\text{-}eff}}(T)$ initially appears below 37 K, which corresponds to the T_{FE} of the strained layer (Fig. 2(b)), but disappears below 32 K, indicating that E_{pol} is not large enough to pole the strained layer. A second onset of $P_{\mathrm{r\text{-}eff}}(T)$ appears at 25 K (T_{FE} of the relaxed layer), which corresponds to the

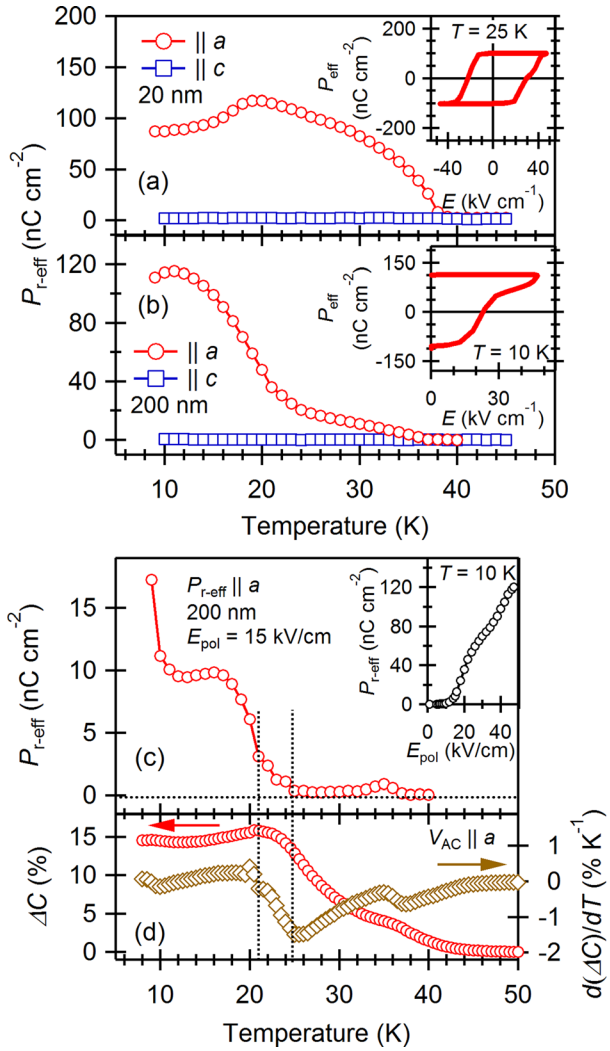

FIG. 3. Temperature dependent $P_{\mathrm{r\text{-}eff}}$ of (a) the 20 nm and (b) the 200 nm *o*-HMO film derived from FE hysteresis curves using $E_{\mathrm{pol}} = 47$ kV cm^{-1}. A part of the FE hysteresis curve is shown in the insets. (c) The $P_{\mathrm{r\text{-}eff}}(T)$ of the 200 nm *o*-HMO film derived from FE hysteresis curves using $E_{\mathrm{pol}} = 15$ kV cm^{-1}. The $P_{\mathrm{r\text{-}eff}}$ at 10 K is plotted as a function of E_{pol} in the inset. (d) The normalized capacitance and its derivative with respect to temperature along the *a*-axis.

temperature at which the slope of $\Delta C(T)$ becomes steepest (Fig. 3(d)). This feature was also observed in bulk polycrystalline *o*-HMO by Lorenz *et al.*[22,23] and its physical origin is still under debate. The $P_{\mathrm{r\text{-}eff}}(T)$ shows a jump at 21 K where ΔC shows a small hump, indicating a two-step FE transition in the relaxed *o*-HMO. These are first order transitions as revealed by the thermal hysteresis in $\Delta C(T)$ (Fig. 2(d)). The orientation of P_{eff} of the relaxed layer is along the *a*-axis, unlike that of single crystals, reported along the *c*-axis.[20] This difference may be due to an interfacial interaction between the relaxed and the strained layer, or that *a*-axis polarization is an intrinsic property, as was theoretically predicted.[45]

The large alteration in T_{FE} of the strained layer implies a change in magnetic properties. To observe differences in magnetic order between the two layers, we employed RSXD. Fig. 4 presents the (0 q_b 0) magnetic reflection from a 32 nm (strained) and a 120 nm (relaxed) *o*-HMO film. The correlation length[46] calculated from the FWHM of the curve is

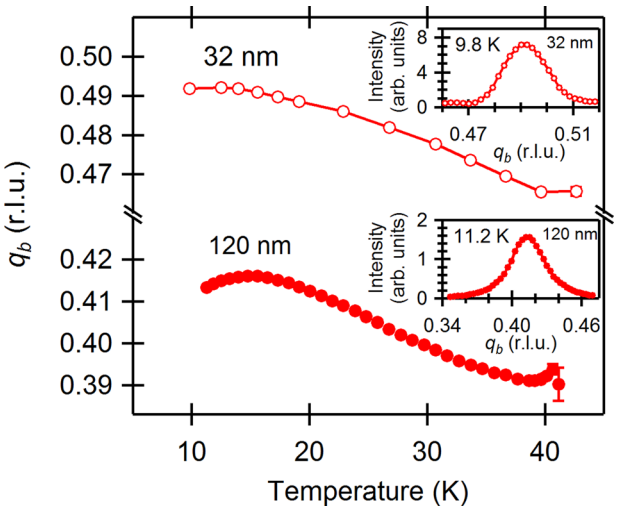

FIG. 4. Temperature dependence of the magnetic modulation parameter q_b derived from (0 q_b 0) reflections of a 32 nm (open symbols) and a 120 nm (closed symbols) film. The (0 q_b 0) reflection at a selected temperature is shown in the insets.

~32 nm, in the order of the probe depth. Since the critical thickness is around 30 nm, we may argue that the measurement on the 120 nm film probes the magnetic properties of the relaxed (top) layer only. The integrated intensities of the (0 q_b 0) reflection as functions of temperature (not shown) indicate that the Néel temperature of the Mn magnetic order of the strained and the relaxed layers are 41 K and 39 K, respectively. The influence of compressive strain along the *a*-axis is reflected in the magnitude of q_b, presented in Fig. 4 as function of temperature. The strained *o*-HMO film exhibits a much larger q_b for the whole measured temperature range compared to that of the relaxed *o*-HMO, which corresponds to bulk values.[20,25] Thus, the compressive strain modifies the magnetic modulation vector (0 q_b 0), pushing q_b closer to commensurate E-type ordering (from $q_b \approx 0.41$ to ≈ 0.49 at ~10 K). However, pure commensurate magnetic ordering was not observed from the (0 q_b 0) reflection, in agreement with reports for other *o*-*RE*MnO_3 films.[39,47,48]

It is thus demonstrated that the compressively strained *o*-HMO films acquire two key differences in their multiferroic properties with respect to relaxed films and to bulk: an increased value of the T_{FE}, and an enlarged magnetic modulation q_b, which is close to the commensurate E-type value of 0.5. It is reasonable to argue that these significant differences are a consequence of the modification of interatomic distances by epitaxial strain. In particular, the e_g state of Jahn-Teller distorted MnO_6 octahedra in the *ab*-plane may be strongly influenced since the aspect ratio of the unit cell in the *ab*-plane (*b*/*a*) is changed by 2.2%. Considering that the spin ordering of *o*-*RE*MnO_3 is realized by a subtle interplay of exchange interactions, even a small shift of interatomic distances can lead to changes in transition temperatures and stabilize different magnetic ordering schemes.

In summary, we investigated lattice, electric, and magnetic properties of *o*-HMO films grown on YAO (010) substrates. *o*-HMO films grow coherently on the substrate up to a thickness of ~30 nm, and an additional relaxed layer forms on top for thicker films, which exhibits strain relaxation with respect to thickness. Electrical characterization and RSXD measurements reveal significant differences in the multiferroic properties of strained and relaxed films. The strained film exhibits $T_{FE} = 37.5$ K, which is notably higher than bulk and relaxed *o*-HMO films (~25 K). The magnetic ordering vector (0 q_b 0) shifts significantly from $q_b \approx 0.41$ for bulk and the relaxed films to ~0.49 for the strained films. This modification of electric and magnetic ordering may be attributed to changes in interatomic distances, induced by compressive strain along the *a*-axis.

Financial support and CROSS funding to K.S. from PSI are gratefully acknowledged. We would like to thank D. Marty (PSI, Laboratory for Micro- and Nanotechnology) for support with optical lithography and U. Greuter for the implementation of a Sawyer-Tower circuit for ferroelectric hysteresis measurements. The use of the LCR-meter belonging to the Laboratory for Scientific Developments and Novel Materials is acknowledged. Y.W.W. and M.R. are supported through Grants from the Swiss National Science Foundation No. 200020-159220 and a Sinergia Grant No. 200021-137657, respectively. E.M.B. and L.R. are supported by the NCCR MUST from the Swiss National Science Foundation. E.M.B. acknowledges funding from the European Community's Seventh Framework Program (FP7/2007-2013) under Grant Agreement No. 290605 (COFUND: PSI-FELLOW). Soft x-ray experiments were performed at the X11MA beamline at SLS, whose beamline staff we gratefully acknowledge.

[1]L. W. Martin and D. G. Schlom, Curr. Opin. Solid State Mater. Sci. **16**, 199 (2012).
[2]C. A. F. Vaz, J. Phys.: Condens. Matter **24**, 333201 (2012).
[3]M. Trassin, J. Phys.: Condens. Matter **28**, 033001 (2016).
[4]C. Lu, W. Hu, Y. Tian, and T. Wu, Appl. Phys. Rev. **2**, 021304 (2015).
[5]T. Suzuki, Y. Nishi, and M. Fujimoto, Philos. Mag. A **79**, 2461 (1999).
[6]Y. B. Chen, H. P. Sun, M. B. Katz, X. Q. Pan, K. J. Choi, H. W. Jang, and C. B. Eom, Appl. Phys. Lett. **91**, 252906 (2007).
[7]M. Kawai, D. Kan, S. Isojima, H. Kurata, S. Isoda, Y. Shimakawa, S. Kimura, and O. Sakata, J. Appl. Phys. **102**, 114311 (2007).
[8]H. P. Sun, X. Q. Pan, J. H. Haeni, and D. G. Schlom, Appl. Phys. Lett. **85**, 1967 (2004).
[9]C. Merckling, M. El-Kazzi, G. Delhaye, V. Favre-Nicolin, Y. Robach, M. Gendry, G. Grenet, G. Saint-Girons, and G. Hollinger, J. Cryst. Growth **306**, 47 (2007).
[10]A. J. Grutter, F. J. Wong, C. A. Jenkins, E. Arenholz, A. Vailionis, and Y. Suzuki, Phys. Rev. B **88**, 214410 (2013).
[11]A. Grutter, F. Wong, E. Arenholz, M. Liberati, A. Vailionis, and Y. Suzuki, Appl. Phys. Lett. **96**, 082509 (2010).
[12]D. Kan, R. Aso, H. Kurata, and Y. Shimakawa, J. Appl. Phys. **113**, 173912 (2013).
[13]K. J. Choi, M. Biegalski, Y. L. Li, A. Sharan, J. Schubert, R. Uecker, P. Reiche, Y. B. Chen, X. Q. Pan, V. Gopalan, L.-Q. Chen, D. G. Schlom, and C. B. Eom, Science **306**, 1005 (2004).
[14]J. H. Haeni, P. Irvin, W. Chang, R. Uecker, P., Reiche, Y. L. Li, S. Choudhury, W. Tian, M. E. Hawley, B. Craigo, A. K. Tagantsev, X. Q. Pan, S. K. Streiffer, L. Q. Chen, S. W. Kirchoefer, J. Levy, and D. G. Schlom, Nature **430**, 758 (2004).
[15]Y. Konishi, Z. Fang, M. Izumi, T. Manako, M. Kasai, H. Kuwahara, M. Kawasaki, K. Terakura, and Y. Tokura, J. Phys. Soc. Jpn. **68**, 3790 (1999).
[16]J. H. Lee, L. Fang, E. Vlahos, X. Ke, Y. W. Jung, L. F. Kourkoutis, J.-W. Kim, P. J. Ryan, T. Heeg, M. Roeckerath, V. Goian, M. Bernhagen, R. Uecker, P. C. Hammel, K. M. Rabe, S. Kamba, J. Schubert, J. W. Freeland, D. A. Muller, C. J. Fennie, P. Schiffer, V. Gopalan, E. Johnston-Halperin, and D. G. Schlom, Nature **466**, 954 (2010); **476**, 114 (2011).
[17]H. Katsura, N. Nagaosa, and A. V. Balatsky, Phys. Rev. Lett. **95**, 057205 (2005).
[18]M. Mochizuki, N. Furukawa, and N. Nagaosa, Phys. Rev. B **84**, 144409 (2011).

[19]S. Ishiwata, Y. Kaneko, Y. Tokunaga, Y. Taguchi, T.-H. Arima, and Y. Tokura, Phys. Rev. B **81**, 100411 (2010).
[20]N. Lee, Y. J. Choi, M. Ramazanoglu, W. Ratcliff II, V. Kiryukhin, and S.-W. Cheong, Phys. Rev. B **84**, 020101 (2011).
[21]S. M. Feng, Y. S. Chai, J. L. Zhu, N. Manivannan, Y. S. Oh, L. J. Wang, Y. S. Yang, C. Q. Jin, and K. H. Kim, New J. Phys. **12**, 073006 (2010).
[22]B. Lorenz, Y. Q. Wang, Y. Y. Sun, and C. W. Chu, Phys. Rev. B **70**, 212412 (2004).
[23]B. Lorenz, Y.-Q. Wang, and C.-W. Chu, Phys. Rev. B **76**, 104405 (2007).
[24]A. Muñoz, M. T. Casáis, J. A. Alonso, M. J. Martínez-Lope, J. L. Martínez, and M. T. Fernández-Díaz, Inorg. Chem. **40**, 1020 (2001).
[25]H. W. Brinks, J. Rodoríguez-Carvajal, H. Fjellvåg, A. Kjekshus, and B. C. Hauback, Phys. Rev. B **63**, 094411 (2001).
[26]H. W. Brinks, H. Fjellvåg, and A. Kjekshus, J. Solid State Chem. **129**, 334 (1997).
[27]A. Muñoz, J. A. Alonso, M. T. Casais, M. J. Martínez-Lope, J. L. Martínez, and M. T. Fernández-Díaz, J. Phys.: Condens. Matter **14**, 3285 (2002).
[28]S. Ishiwata, Y. Tokunaga, Y. Taguchi, and Y. Tokura, J. Am. Chem. Soc. **133**, 13818 (2011).
[29]D. Okuyama, S. Ishiwata, Y. Takahashi, K. Yamauchi, S. Picozzi, K. Sugimoto, H. Sakai, M. Takata, R. Shimano, Y. Taguchi, T. Arima, and Y. Tokura, Phys. Rev. B **84**, 054440 (2011).
[30]M. Nakaumra, Y. Tokunaga, M. Kawasaki, and Y. Tokura, Appl. Phys. Lett. **98**, 082902 (2011).
[31]X. Martí, V. Skumryev, V. Laukhin, F. Sánchez, M. García-Cuenca, C. Ferrater, M. Varela, and J. Fontcuberta, J. Mater. Res. **22**, 2096 (2007).
[32]I. Fina, L. Fàbrega, X. Martí, F. Sánchez, and J. Fontcuberta, Appl. Phys. Lett. **97**, 232905 (2010).
[33]X. Martí, I. Fina, V. Skumryev, C. Ferrater, M. Varela, L. Fàbrega, F. Sánchez, and J. Fontcuberta, Appl. Phys. Lett. **95**, 142903 (2009).
[34]J. A. Alonso, M. J. Martínez-Lope, M. T. Casais, and M. T. Fernández-Díaz, Inorg. Chem. **39**, 917 (2000).
[35]M. C. Morris, H. F. McMurdie, E. H. Evans, B. Paretzkin, H. S. Parker, N. P. Pyrros, and C. R. Hubbard, "Aluminum Yttrium Oxide, $AlYO_3$," Natl. Bur. Stand. (U.S.), Monograph No. 25, 19, 7 (U.S. Government Printing Office, 1982).
[36]M. Fukunaga and Y. Noda, J. Phys. Soc. Jpn. **77**, 064706 (2008).
[37]U. Staub, V. Scagnoli, Y. Bodenthin, M. García-Fernández, R. Wetter, A. M. Mulders, H. Grimmer, and M. Horisberger, J. Synchrotron Radiat. **15**, 469 (2008).
[38]U. Flechsig, F. Nolting, A. Fraile Rodoríguez, J. Krempaský, C. Quitmann, T. Schmidt, S. Spielmann, and D. Zimoch, AIP Conf. Proc. **1234**, 319 (2010).
[39]Y. W. Windsor, M. Ramakrishnan, L. Rettig, A. Alberca, E. M. Bothschafter, U. Staub, K. Shimamoto, Y. Hu, T. Lippert, and C. W. Schneider, Phys. Rev. B **91**, 235144 (2015).
[40]V. Yu Pomjakushin, M. Kenzelmann, A. Dönni, A. B. Harris, T. Nakajima, S. Mitsuda, M. Tachibana, L. Keller, J. Mesot, H. Kitazawa, and E. Takayama-Muromachi, New J. Phys. **11**, 043019 (2009).
[41]L. J. Wang, Y. S. Chai, S. M. Feng, J. L. Zhu, N. Manivannan, C. Q. Jin, Z. Z. Gong, X. H. Wang, and L. T. Li, J. Appl. Phys. **111**, 114103 (2012).
[42]B. Xu, R. G. Polcawich, S. Trolier-McKinstry, Y. Ye, L. E. Cross, J. J. Bernstein, and R. Miller, Appl. Phys. Lett. **75**, 4180 (1999).
[43]Q. Zhang, S. Gross, S. Tadigadapa, T. Jackson, F. Djuth, and S. Trolier-McKinstry, Sens., Actuators A **105**, 91 (2003).
[44]C. M. Folkman, S. H. Baek, C. T. Nelson, H. W. Jang, T. Tybell, X. Q. Pan, and C. B. Eom, Appl. Phys. Lett. **96**, 052903 (2010).
[45]S. Picozzi, K. Yamauchi, B. Sanyal, I. A. Sergienko, and E. Dagotto, Phys. Rev. Lett. **99**, 227201 (2007).
[46]S. B. Wilkins, P. D. Hatton, M. D. Roper, D. Prabhakaran, and A. T. Boothroyd, Phys. Rev. Lett. **90**, 187201 (2003).
[47]H. Wadati, J. Okamoto, M. Garganourakis, V. Scagnoli, U. Staub, Y. Yamasaki, H. Nakao, Y. Murakami, M. Mochizuki, M. Nakamura, M. Kawasaki, and Y. Tokura, Phys. Rev. Lett. **108**, 047203 (2012).
[48]Y. W. Windsor, S. W. Huang, Y. Hu, L. Rettig, A. Alberca, K. Shimamoto, V. Scagnoli, T. Lippert, C. W. Schneider, and U. Staub, Phys. Rev. Lett. **113**, 167202 (2014).